Isonitrile biosynthesis by non-heme iron(II)-dependent oxidases/decarboxylases

Antonio Del Rio Flores, Rui Zhai, and Wenjun Zhang*

Department of Chemical and Biomolecular Engineering, University of California, Berkeley, CA, United States

*Corresponding author. e-mail address: wjzhang@berkeley.edu

Contents

1.	Introduction	144
2.	Enzyme expression, purification, and in vitro assays with ScoE	147
	2.1 Expression of protein	147
	2.2 Purification of soluble protein	148
	2.3 Chemical synthesis of substrate and product	149
	2.4 Substrate and product detection assays	152
	2.5 Kinetic characterization of ScoE	156
3.	Mechanistic dissection of isonitrile formation using spectroscopic methods	156
	3.1 NMR analyses of <i>in vitro</i> biochemical assays for detection of intermediates	156
	3.2 Chemical synthesis of reaction intermediates and shunt products	159
	3.3 LC-HRMS detection of intermediates and shunt products	161
	3.4 Kinetic and quantitative dissection of on-pathway and off-pathway species	163
4.	Enzyme expression, purification, and in vitro assays with Rv0097	165
	4.1 Expression and purification of soluble protein	165
	4.2 Chemical synthesis of substrate	165
	4.3 Enzymatic synthesis of substrates	166
	4.4 Product detection assays	167
	4.5 Kinetic characterization of Rv0097	167
5.	Perspectives	168
Ac	knowledgments	169
Re	References	

Abstract

The isonitrile group is a compact, electron-rich moiety coveted for its commonplace as a building block and bioorthogonal functionality in synthetic chemistry and chemical biology. Hundreds of natural products containing an isonitrile group with intriguing bioactive properties have been isolated from diverse organisms. Our recent discovery of a conserved biosynthetic gene cluster in some Actinobacteria species highlighted a novel enzymatic pathway to isonitrile formation involving a non-heme

iron(II) and α -ketoglutarate-dependent dioxygenase. Here, we focus this chapter on recent advances in understanding and probing the biosynthetic machinery for isonitrile synthesis by non-heme iron(II) and α -ketoglutarate-dependent dioxygenases. We will begin by describing how to harness isonitrile enzymatic machinery through heterologous expression, purification, synthetic strategies, and *in vitro* biochemical/kinetic characterization. We will then describe a generalizable strategy to probe the mechanism for isonitrile formation by combining various spectroscopic methods. The chapter will also cover strategies to study other enzyme homologs by implementing coupled assays using biosynthetic pathway enzymes. We will conclude this chapter by addressing current challenges and future directions in understanding and engineering isonitrile synthesis.

1. Introduction

The isonitrile synthon is an electron-rich functional group that behaves as a bioactive warhead for many naturally derived specialized metabolites. To date, more than two hundred isonitrile-containing natural products have been identified from marine and terrestrial sources and have exhibited a broad range of properties that drive virulence, metal acquisition, detoxification, and antimicrobial phenotypes (Clarke-Pearson & Brady, 2008; Crawford, Portmann, Zhang, Roeffaers, & Clardy, 2012; Del Rio Flores, Barber, et al., 2022; Matsuda, Maruyama, Imachi, Ikeda, & Wakimoto, 2024; Wang et al., 2017). Apart from its presence in naturally occurring compounds, the isonitrile moiety is ubiquitous in synthetic chemistry and chemical biology owing to its ability of promoting versatile chemistry as both an electrophile and nucleophile (Zhang, Evanno, & Poupon, 2020). Isonitriles behave as carbon monoxide analogs due to their ability to participate in π -back bonding with metal atomic orbitals, and engage in multi-component reactions, such as the Passerini and Ugi reactions (La Pierre, Arnold, Bergman, & Toste, 2012; Ugi, Werner, & Domling, 2003; Wang, Wang, & Zhu, 2018; Zhi, Ma, & Zhang, 2019). One of the key features of the isonitrile moiety that makes it an ideal candidate for bioorthogonal chemistry is its compact structure, stability in biology media, and relative ease to synthesize through traditional synthetic methods (Del Rio Flores, Barber, et al., 2022). The isonitrile is known to be involved in bioorthogonal reactions with chlorooximes (Schäfer et al., 2019) and the [4 + 1] cycloaddition reaction with tetrazines (Imming, Mohr, Muller, Overheu, & Seitz, 1982; Stockmann, Neves, Stairs, Brindle, & Leeper, 2011; Tu et al., 2019).

In contrast to the broad utility of isonitrile in various scientific disciplines, only a handful of enzymes have been biochemically characterized for isonitrile construction. The first biosynthetic route to isonitriles is represented

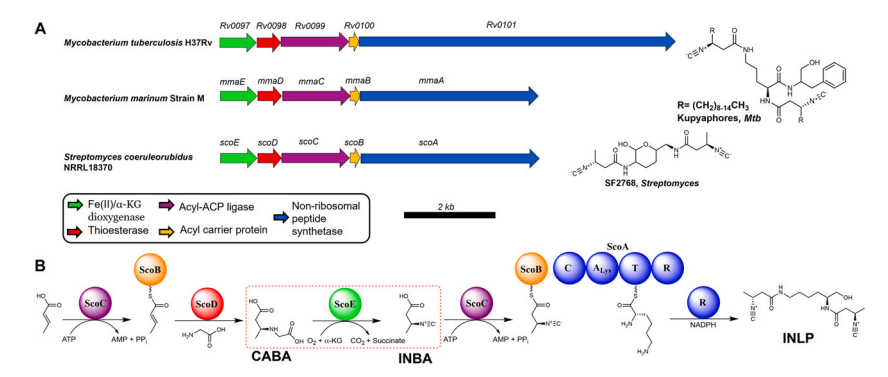


Fig. 1 Biosynthesis of isonitrile lipopeptides (INLPs) from actinobacteria. (A) Conserved INLP biosynthetic gene clusters with their corresponding metabolites. (B) Proposed biosynthetic pathway of INLP biosynthesis from *Streptomyces coeruleorubidus*. The ScoE reaction is boxed in red with primary substrate CABA and primary product INBA.

by the IsnA synthase family that catalyze the condensation reaction between ribulose-5-phosphate and the α -amino group of tryptophan or tyrosine (Brady & Clardy, 2005; Brady, Chao, Handelsman, & Clardy, 2001; Chang et al., 2017; Drake & Gulick, 2008). Our group discovered the second known route to isonitrile in nature by studying a non-ribosomal peptide synthetase (NRPS)-encoding gene cluster (Rv0097-Rv0101) from Mycobacterium tuberculosis (Mtb) (Fig. 1A). Notably, many biological studies supported the notion that a virulence factor is produced by the gene cluster, however the responsible metabolite was not identified (Harris et al., 2017). Genome mining efforts also revealed that homologs of Rv0097-Rv0101 were conserved among pathogenic Mycobacteria and also found from other genera such as Streptomyces, Nocardia, Rhodococcus, and Kutzneria. The association of this gene cluster with virulence warranted further metabolic exploration to understand and elucidate the function of the five corresponding genes. The function of the five homologous genes from Streptomyces coeruleorubidus (scoA-E) was elucidated through reconstitution in E. coli resulting in the production of a family of isonitrile lipopeptides (INLPs) similar to the known antibiotic SF2768 (Harris et al., 2017; Wang et al., 2017) (Fig. 1B). The INLP pathway starts with ScoC, an acyl-acyl carrier protein (ACP) ligase that activates and loads crotonic acid on ScoB, an ACP (Fig. 1B). ScoD, a thioesterase homolog, then catalyzes both the Michael addition of glycine to the β-position of crotonoyl- S-ScoB and hydrolysis off the ACP to yield (R)-3-((carboxymethyl)amino)butanoic acid (CABA).

CABA serves as the substrate for ScoE, a non-heme iron(II) and α -keto-glutarate-dependent dioxygenase (Fe(II)/ α -KG-dioxygenase), that catalyzes oxidative decarboxylation to synthesize (R)-3-isocyanobutanoic acid (INBA) (Fig. 1B). ScoC acts again in the pathway to activate and load INBA onto ScoB, where the β -isonitrile moiety becomes condensed by both amino groups of lysine promoted by the single-module NRPS ScoA. The last step involves a four-electron reductive release from ScoA to form the INLP with a terminal alcohol (Harris et al., 2017) (Fig. 1B), or a two-electron reductive release followed by cyclization to yield SF2768 with a tailoring enzyme (Wang et al., 2017). Notably, recent reports have shown that *Mycobacterium tuberculosis* produces similar INLPs, termed kupyaphores, that play a critical role in promoting metal acquisition (Buglino, Ozakman, Xu, Chowdhury, & Glickman, 2022; Mehdiratta et al., 2022).

Fe(II)/α-KG-dioxygenases represent the largest subgroup of mononuclear non-heme iron enzymes and are known to catalyze a myriad of oxidative transformations such as hydroxylation, epoxidation, desaturation, halogenation, and among others (Martinez & Hausinger, 2015). These enzymes possess a conserved double-stranded β -helix fold that resembles a barrel-like structure. The mononuclear Fe(II) is coordinated by a conserved 2-His-1-carboxylate facial triad at one end of the barrel, thus leaving three vacant binding sites for molecular oxygen and the bidentate ligand α-KG (Ushimaru & Abe, 2023). The carboxylate residue is replaced with an alanine/glycine residue in the halogenases, thus freeing a coordination site for the halide ion (Blasiak, Vaillancourt, Walsh, & Drennan, 2006). When molecular oxygen binds to the mononuclear Fe(II) cofactor, a Fe (III)-superoxo species is formed where the distal oxygen attacks C2 of α -KG to form a peroxohemiketal bicyclic intermediate that undergoes oxidative cleavage to release CO2, succinate, and a high-valent Fe(IV)=O species that mediates oxidation chemistry (Bollinger, Price, Hoffart, Barr, & Krebs, 2005; Grzyska, Appelman, Hausinger, & Proshlyakov, 2010; Martinez & Hausinger, 2015). The Fe(IV)=O species abstracts a hydrogen atom from the primary substrate to yield an Fe(III)-OH species and a substrate radical (Price, Barr, Glass, Krebs, & Bollinger, 2003). For a typical hydroxylation reaction, the hydroxyl group is rebounded to the primary substrate via a recombination event between the Fe(III)-OH and substrate radical (Bollinger et al., 2005; Martinez & Hausinger, 2015; Price et al., 2003). Despite the diverse repertoire of oxidative transformations reported by Fe(II)/ α -KG-dioxygenases, isonitrile formation represents a novel activity within this enzyme superfamily that poses profound mechanistic rigor.

Most enzymes in this superfamily catalyze two-electron oxidation reactions of the primary substrate, while the conversion from CABA to INBA involves a four-electron oxidation leading to a fully oxidized functionality. In this chapter, we begin by describing general methods for gene expression, protein purification, synthetic methods, and *in vitro* biochemical assays. This discussion will resume by examining general strategies to dissect the reaction mechanism of isonitrile formation by combining spectroscopy techniques and detailed kinetic characterization of pathway intermediates/shunt products. Then, we will discuss a generalizable strategy to study ScoE homologs based on our recent work on Mycobacterial enzymes. We will conclude this work by addressing current challenges and future directions in the field. The relevant publications from our laboratory are highlighted here to allow for better accessibility to the reader (Del Rio Flores et al., 2023; Del Rio Flores, Barber, et al., 2022; Del Rio Flores, Kastner, et al., 2022; Huang, Cai, Del Rio Flores, Twigg, & Zhang, 2019; Jonnalagadda et al., 2021).



2. Enzyme expression, purification, and in vitro assays with ScoE

2.1 Expression of protein

Since the native organism of ScoE is underdeveloped for protein expression and purification, a heterologous host is routinely utilized to obtain active enzyme (Harris et al., 2018). Escherichia coli is one of the most widely utilized heterologous expression hosts for recombinant protein production owing to its genetic tractability, fast doubling time, and well-characterized primary metabolism (Gu & Zhang, 2022; Rosano & Ceccarelli, 2014; Zhu & Zhang, 2018). The commercially available strain E. coli BL21 (DE3) along with pET vectors are typically utilized for heterologous expression of hexahistidinetagged recombinant protein (Studier & Moffatt, 1986). Some commonly utilized pET vectors include pET30 that contains an N-terminal hexahistidine tag, pET24b that contains a C-terminal hexahistidine tag, and pET28a that contains both N- and C-terminal hexahistidine tags. The gene of interest can be cloned into these vectors under an inducible, strong T7 promoter through either Gibson, restriction enzyme-dependent, or ligation-independent cloning approaches. A T7 RNA polymerase under an isopropyl β-D-1-thiogalactopyranoside (IPTG)-inducible lacUV5 promoter is encoded within the genome of E. wli BL21 (DE3) and is required to express target recombinant proteins cloned into the pET vectors.

A general procedure for protein purification is outlined here for isolation of ScoE. The plasmid containing scoE is transformed into chemically competent E. coli BL21 (DE3) via heat-shock transformation at 42 °C. A single colony is picked from lysogeny broth (LB) agar plates containing the appropriate antibiotic and grown in a 10 mL starter culture of LB containing antibiotics at 37 °C for an overnight period. For long-term storage, a glycerol stock is prepared by aliquoting 1 mL of the overnight culture in 10% glycerol and stored at -80 °C in a cryovial. The remaining starter culture is utilized to inoculate 1 L of LB supplemented with appropriate antibiotics (~1% inoculation ratio). The culture is placed inside a shaker at 250 rpm at 37 °C until an optical density at 600 nm (OD₆₀₀) of 0.5–0.6 is measured. The shake flask is then placed on ice for 10 min, followed by addition of 120 µM IPTG to induce protein expression. The induced culture is then placed back inside the shaker at 200 rpm for 16 h at 16 °C. To optimize protein expression, it is common for researchers to adjust culture time and temperature, IPTG concentration, and inducing at different OD_{600} .

2.2 Purification of soluble protein

The E. coli cultures are harvested by centrifugation at ~6000 x g at 4 °C for 15 min and the supernatant is removed (Jonnalagadda et al., 2021). If protein purification is not desired to be carried out the same day, the cell pellet is transferred to a 50 mL conical tube and flash frozen in liquid nitrogen before stored at -80 °C. Continuing with the purification method, the cell pellet is resuspended in 30 mL of lysis buffer (25 mM 4-(2hydroxyethyl)-1-piperazineethanesulfonic acid (HEPES) pH 8.0, 500 mM sodium chloride (NaCl), 5 mM imidazole) and lysed by sonication in an ice-water bath. The cell debris is pelleted using centrifugation at 27,000 x g at 4 °C for 1 h, and the supernatant is filtered with a 0.45 µm filter before batch binding. Nickel-nitrilotriacetic acid (Ni-NTA) agarose resin is then added to the clarified, filtered lysate (1.5 mL/L of culture) and nutated at 4 °C for 1 h. The protein/resin mixture is then loaded onto a gravity flow column and the flowthrough is discarded. For a 1 L culture, the column is then washed with approximately 25 mL of wash buffer (25 mM HEPES pH 8.0, 100 mM NaCl, 20 mM imidazole) and the target protein is eluted in approximately 15 mL of elution buffer (25 mM HEPES pH 8.0, 100 mM NaCl, 250 mM imidazole). The complete process is monitored using a Bradford assay. Purified proteins are concentrated using 10 kDa molecular weight cutoff (MWCO) Amicon Ultra spin filters to yield 3 mL of protein.

ScoE is then dialyzed at 4 °C using a 10 kDa Slide-A-Lyzer Dialysis Cassette in 1 L of dialysis buffer (25 mM HEPES pH 8.0, 100 mM NaCl, 1 mM ethylenediaminetetraacetic acid (EDTA)) to yield apo protein which is more stable. We observed that purified protein that is not dialyzed is less active than apo protein that is reconstituted with fresh iron. The decreased activity of this protein becomes more drastic if stored at – 80 °C for a few days. The dialysis buffer was changed twice over 9 h and dialyzed overnight. ScoE is concentrated the next morning using a 10 kDa MWCO Amicon Ultra spin filter until the protein concentration reaches 40 mg/mL and 10% v/v glycerol is added. The proteins are flash frozen in liquid nitrogen and stored at – 80 °C. Depending on different expression levels, the purity of ScoE ranges from ~70 to 90% according to sodium dodecyl sulfate—polyacrylamide gel electrophoresis (SDS-PAGE).

Ion exchange and size exclusion chromatography can be employed to further purify resulting protein.

2.3 Chemical synthesis of substrate and product

The native substrate of ScoE (CABA) is not commercially available, therefore it needs to be synthesized prior to conducting biochemical assays (Harris et al., 2018). Similarly, the ScoE reaction product (INBA) can be synthesized as a chemical standard or for quantification purposes (Fig. 2). The precursors and solvents are acquired from commercial vendors, including Ark Pharm Inc., Sigma-Aldrich, and Cambridge Isotope Laboratories. Please note that appropriate personal protective equipment must be utilized to minimize exposure to potential hazards from synthetic chemistry. Our synthetic experiments require wearing a properly fitted lab coat, safety goggles, and nitrile gloves. All the synthetic steps discussed in this chapter should be conducted in a well-ventilated fume hood. (R)-3-aminobutanoic acid (0.52 g, 5 mmol) is first dissolved in a solution of water (10 mL) and tertbutyl alcohol (15 mL) in a round bottom flask. Sodium carbonate (1.59 g, 15 mmol) and di-tert-butyl dicarbonate (1.64 g, 7.5 mmol) are then added sequentially to the solution. The reaction is stirred and refluxed for 2 h at 210 °C. The mixture is cooled to 0 °C in an ice bath and acidified with 6 N HCl to pH 1.0. The tert-butyl alcohol is removed in vacuo using a rotary evaporator and the aqueous phase is extracted with ethyl acetate 3 times. The organic fractions are combined and washed with water, brine and then dried over sodium sulfate (Na₂SO₄) anhydrous. The resulting solvent was then removed to yield N-Boc-(R)-3-aminobutanoic acid that resembles a colorless oily liquid. The crude product is then dissolved in acetone (10 mL),

Fig. 2 Synthetic schemes for (*R*)-3-((carboxymethyl)amino)butanoic acid (CABA) and (*R*)-3-isocyanobutanoic acid (INBA).

then triethylamine (1.4 mL, 10 mmol) and benzyl bromide (0.7 mL, 5.5 mmol) are added dropwise. The reaction is stirred overnight at room temperature. Water is added the next morning to quench the reaction. The acetone is next removed in *vacuo* through rotary evaporation. The aqueous phase is extracted with ethyl acetate 3 times. The organic fractions are combined and washed with water, brine and then dried over Na₂SO₄. The solvent is removed to yield benzyl-*N*-Boc-(*R*)-3-aminobutanoic acid (**C1**) as a colorless oily liquid. The product is purified by flash silica chromatography using a mobile phase of 100% hexanes initially and increasing ethyl acetate composition in 10% increments. Fractions containing **C1** are identified with liquid chromatography high-resolution mass spectrometry (LC-HRMS).

C1 (290 mg, 1 mmol) is dissolved in dichloromethane (10 mL) and cooled to $0\,^{\circ}$ C in an ice bath. Trifluoroacetic acid (TFA, 5 mL) is then added dropwise. These steps should be conducted inside a well-ventilated fume hood. The mixture is then allowed to warm to room temperature and stirred for 2 h and monitored by thin liquid chromatography (TLC). The solvent is then removed *in vacuo* using a rotary evaporator to yield benzyl-(R)-3-aminobutanoic acid (C2) as a colorless oily liquid.

C2 (193 mg, 1 mmol) is dissolved in a mixture of acetonitrile (5 mL) and potassium carbonate (208 mg, 1.5 mmol), then tert-butyl-bromoacetate (234 mg, 1.2 mmol) is added. The reaction is stirred overnight at room temperature. The organic solvent is removed *in vacuo* using a rotary evaporator and the aqueous phase is extracted with ethyl acetate 3 times. The organic fractions are combined and washed with water, brine and then dried over Na₂SO₄, and the solvent was removed to yield crude benzyl-(*R*)-3-((2-(tert-butoxy)-2-oxoethyl)amino)butanoate (C3). The crude product is purified using HPLC to yield C3, a colorless oily liquid.

C3 (307 mg, 1 mmol) is first dissolved in ethanol and 10% Pd/C (15 mg) is sequentially added. The reaction is stirred under a hydrogen atmosphere (1 atm) at room temperature for 2 h. The hydrogen atmosphere can be done by filling a balloon with hydrogen gas and utilizing a long needle to bubble gas through a rubber septum. The solvent is then removed *in vacuo* using a rotary evaporator to yield (R)-3-((2-(tert-butoxy)-2-oxoethyl)amino)butanoate (C4), a colorless oily liquid.

C4 is dissolved in dichloromethane (10 mL) and cooled to 0 °C in an ice bath, and TFA (5 mL) is added dropwise. The mixture is allowed to warm to room temp and stirred for 2 h and monitored by TLC. Solvent is removed *in vacuo* using a rotary evaporator to yield CABA, a colorless oily liquid. CABA is stably stored at -20 °C as an oil or reconstituted in water.

A round flask containing a magnetic stirrer is charged with 2 mmol C2, 20 mL ethyl formate and 3 mmol triethylamine. The reaction mixture is refluxed overnight using a condenser. After cooling the reaction back down to room temperature, the solvent was removed by rotatory evaporation and 20 mL of dichloromethane (DCM) was added to the residue. The organic layer is washed with water and brine twice, respectively. The organic layer is then dried with anhydrous Na₂SO₄ and concentrated by rotatory evaporation to get the crude product. The pure product was separated by silica gel with DCM:Methanol (MeOH) to yield benzyl (*R*)-3-formamidobutanoate (I1), a colorless liquid (65% yield).

A round flask with a magnetic stirrer is charged with 1.0 mmol **I1**, 2.7 mmol triethylamine and 3 mL DCM. The mixture is stirred at -78 °C under a low flow of N₂. A solution of phosphoryl chloride (1.2 mmol) and DCM (0.5 mL) is added dropwise over 10 min. The reaction mixture is stirred at -78 °C for 1.5 h and monitored by TLC. The reaction is quenched by dropwise addition of a saturated Na₂CO₃ solution (15 mL) that is stirred for 15 min. The reaction mixture is then extracted with DCM three times and the organic layer is dried, concentrated and separated

by flash column chromatography using pure DCM. The compound benzyl (R)-3-isocyanobutanoate (**I2**) was obtained as a colorless liquid (74% yield). This product is kept at -80 °C for long-term storage. Since INBA is unstable after generation and highly toxic, **I2** is kept as a precursor until the user needs to synthesize INBA. **I2** can be easily hydrolyzed to make a freshly prepared solution of INBA for downstream experiments.

I2 is subjected to a hydrolysis reaction using KOH. A round flask equipped with a magnetic stirrer was charged with 0.5 mmol I2, 0.5 mmol KOH, 3 mL THF and 0.6 mL water. The reaction mixture is stirred at room temp for 4–5 h. The organic solvent is then removed in *vacuo* using a rotary evaporator and the residue is redissolved in 10 mL DCM and 10 mL water. The water layer is separated and washed with DCM three times. The water layer is flash frozen with liquid nitrogen and lyophilized to yield INBA (\sim 55% yield). INBA can be stored at -80 °C for about a week, but notable degradation to the formamide can be observed.

2.4 Substrate and product detection assays

2.4.1 Preparation of ScoE for biochemical assays

ScoE must be desalted before use in biochemical assays to remove EDTA since it is a metalloenzyme (Del Rio Flores, Kastner, et al., 2022; Harris et al., 2018; Jonnalagadda et al., 2021). A Bio-Rad Bio-Gel P-6 gel column is equilibrated in exchange buffer containing 25 mM HEPES pH 8.0 and 100 mM NaCl. 50-90 μL of ScoE is desalted to remove EDTA following the manufacturer's protocol. The concentration of ScoE is measured using a nanodrop instrument since the concentration will decrease after the desalting process due to residual buffer in the column. The enzyme should be kept on ice and used immediately for any biochemical assays of interest. Ammonium iron(II) sulfate hexahydrate (NH₄)₂Fe(SO₄)₂ should be supplemented in the corresponding assay to match 90% of the protein concentration. The Fe(II) was supplemented aerobically and used within one hour from preparation to ensure the iron is in the 2 + oxidation state. The experimentalist can further add reducing agents to the assay if desired such as ascorbic acid and dithiothreitol (DTT) to further help maintain Fe in the 2 + oxidation state. We found that adding more iron(II) sulfate hexahydrate to ScoE did not significantly affect catalytic activity, and using too much iron(II) (i.e., 2X more than the protein concentration) resulted in partial precipitation of protein.

2.4.2 In vitro product formation assays

ScoE catalyzes a complex biochemical reaction that is composed of three reactants, mononuclear Fe(II), and various reaction products/intermediates. The most basic biochemical reaction consists of an activity assay for the enzymatic production of INBA (Harris et al., 2018; Jonnalagadda et al., 2021). There are two main ways to test for INBA production by either direct detection INBA or indirectly via a click reaction with tetrazine to generate a stable derivatized product (Del Rio Flores et al., 2023; Del Rio Flores, Kastner, et al., 2022; Harris et al., 2018; Huang, Cai, Del Rio Flores, Twigg, & Zhang, 2020; Jonnalagadda et al., 2021). The indirect method was developed for more reliable quantification of isonitrile formation due to the instability of INBA and ability to use reverse phase chromatography to separate the derivatized product (Del Rio Flores, Kastner, et al., 2022). In short, 3,6-di(pyridine-2-yl)-1,2,4,5-tetrazine (Py-tetrazine) is added in excess to ScoE biochemical assays where it reacts with INBA to generate a universal, stable product known as 3,5-di(pyridine-2-yl)-1H-pyrazol-4-amine (Py-AP) (Huang et al., 2020) that can be used to indirectly test for isonitrile formation and also be used for quantification purposes.

A typical ScoE assay is carried out at room temperature for 15 min in $50\,\mu\text{L}$ of $50\,\text{mM}$ HEPES pH 8.0 containing $0.25\,\text{mM}$ $\alpha\text{-KG}$, $0.5\,\text{mM}$ CABA, $90\,\mu\text{M}$ (NH₄)₂Fe(SO₄)₂ and $100\,\mu\text{M}$ Apo-ScoE. The reaction is mixed gently *via* pipetting. For direct detection of INBA, the reaction is quenched by adding $100\,\mu\text{L}$ cold methanol, centrifuged to remove protein residues, and analyzed using normal phase chromatography (*i.e.*, HILIC column). For the indirect detection of INBA, $100\,\mu\text{L}$ of $667\,\mu\text{M}$ Py-tetrazine dissolved in cold methanol is added to the assay, gently mixed, and incubated for 1 h at room temperature. The reaction mixture is centrifuged to remove aggregated protein and is analyzed using reverse phase chromatography. Isonitrile formation is confirmed by looking for production of Py-AP and comparing the retention time to that of a synthetic standard.

2.4.3 CO₂, CO, formate, and H₂O₂ detection assays

One of the most intriguing facets of isonitrile formation is the fact that the carboxylate on the glycine adduct of CABA is lost during the process to generate INBA (Jonnalagadda et al., 2021). The loss of a carbon unit from CABA can be attributed from CO_2 , CO, or formate release, therefore we developed several assays and spectroscopic methods to probe these mechanistic possibilities. Furthermore, we also aimed to test whether the oxygen utilized in the reaction is fully reduced to water or partially reduced to H_2O_2 .

To detect possible H₂O₂ formation, a 0.5 mL ScoE enzymatic assay was conducted with an integrated oxygen electrode unit (Oxygraph Plus System, Hansatech Instruments, UK). Such instrument has been commonly utilized to study oxygenases/oxidases (Rui et al., 2014). The instrument is calibrated with 0.5 mL of 50 mM HEPES pH 8.0 at room temperature and a mixing rate of 50 RPM. The oxygen signal is equilibrated before addition of $90\,\mu M$ (NH₄)₂Fe(SO₄)₂ with an airtight needle to initiate the reaction. The concentration of oxygen is collected as a function of time, and the reaction is allowed to incubate until the profile reaches a steady state. After the concentration of oxygen reaches an equilibrium, 120 U/mL of catalase is added to the reaction chamber. No appreciable increase of oxygen was observed when compared to controls adding solely water or buffer, indicating that no H₂O₂ was produced from the ScoE enzymatic reaction. H₂O₂ release was also tested using an Amplex Red Hydrogen Peroxide/Peroxidase Assay Kit, which resulted in undetectable peroxide formation in corroboration with the oxygen electrode experiment (Jonnalagadda et al., 2021).

We developed a GC-MS assay to detect gaseous species evolving from the ScoE reaction. Our approach was to chemically synthesize 6-13C-CABA since the loss of C6 would yield reliable results due to the low abundance of ¹³C in Nature. A 4.5 mL reaction mixture containing 50 mM HEPES pH 8.0, 90 μM (NH₄)₂Fe(SO₄)₂, 2 mM 6^{-13} C-CABA, 1 mM α-KG, and 100 μM ScoE was set up in a 10-mL sealed headspace vial (Agilent) and initiated by addition of Fe(II). 1 mL of the headspace gas was acquired using a gastight syringe (Hamilton) and injected into Agilent 5977 A GC-MS system equipped with a HP-5 ms column. The CO₂ and CO signals were confirmed using authentic standards and it was shown that the ScoE biochemical reaction releases CO₂ from the conversion of CABA to INBA. Notably, we also found that ~2 times more ¹³C-CO₂ was produced from biochemical assays using $1,2,3,4^{-13}$ C- α -KG (unlabeled CABA) than with 6^{-13} C-CABA and unlabeled α-KG, respectively. ¹³C-CO was not detected from the GC-MS experiment, thus we conducted an independent experiment to further rule out CO evolution based on a previously reported assay (Warui et al., 2011). A 0.2 mL ScoE enzymatic assay is conducted at room temperature in a sealed tube for 10 min. Myoglobin and sodium dithionite were added at 10 μM and 20 mM final concentrations, respectively, and the reaction mixture was allowed to incubate for 10 min. The septum is immediately removed, and the absorption spectrum is immediately recorded. The Soret band was detected at 434 nm for both controls and reactions, supporting the notion that CO is not produced and in corroboration with GC-MS experiments.

To test for potential formate production from the ScoE reaction, a 200 μ L assay was conducted at room temperature for 10 min and quenched with 400 μ L of cold MeOH. 100 μ L of the supernatant was reacted with 10 μ L of 290 mM 1-ethyl-3-(3-dimethylaminopropyl)carbodiimide and 10 μ L of 120 mM 2-nitrophenylhydrazine (dissolved in 250 mM HCl) (Warui et al., 2011). The reaction was subsequently incubated at 60 °C for 15 min and subjected to LC-HRMS analyses. Additionally, a Sigma-Aldrich Formate Assay Kit was used on the biochemical assay, resulting in no detectable amounts of formate for both independent methods.

The detection of CO_2 instead of the other two carbon equivalents played a pivotal role in uncovering the mechanism of ScoE. The reaction stoichiometry would only be feasible if two equivalents of α -KG were to be consumed to generate one equivalent of isonitrile and three equivalents of CO_2 , with two equivalents of oxygen being fully reduced to water.

2.4.4 Elucidation of reaction stoichiometry

After establishing the substrates and reaction products from the ScoE reaction, the O₂ consumption is quantified by conducting a 0.5 mL assay in an Oxygraph Plus System (Jonnalagadda et al., 2021). The oxygen signal is equilibrated before addition of 90 µM (NH₄)₂Fe(SO₄)₂ with an airtight needle to initiate the reaction. The concentration of oxygen is collected as a function of time, and the reaction is allowed to incubate until the profile reaches a steady state. Two 100 µL aliquots of the reaction mixture are quenched with 200 µL of cold methanol and 200 µL of 667 µM Py-tetrazine dissolved in cold methanol, respectively, to conduct stoichiometry quantification experiments using LC-HRMS. In parallel, 100 µL standards containing 50 mM HEPES pH 8.0 and varying concentrations of CABA, α-KG, Py-AP and succinate are diluted with 200 μL of cold methanol to develop a standard curve using LC-HRMS. Py-AP and CABA are detected and quantified using positive ionization mode, while α -KG and succinate are detected and quantified using negative ionization mode. The analyst must pay careful attention in preparing accurate amounts of each component for quantification and it is recommended to run the standards in parallel with biochemical assays since ionization energies can vary over time when using LC-HRMS. Ultimately, our results indicated that two equivalents of α-KG and oxygen are required to produce one equivalent of INBA. In corroboration, we observed that consumption of CABA and production of INBA is 1:1, respectively, based on the assay conditions described.

2.5 Kinetic characterization of ScoE

The kinetic characterization of ScoE was conducted to determine the parameters for CABA and α -KG, respectively (Harris et al., 2018). Taking the case for CABA, a LC-HRMS assay was designed in which CABA concentration is varied, while the relative amount of α -KG is kept in excess (Harris et al., 2018). Biochemical assays are performed in triplicate in 50 μ L of 50 mM HEPES pH 8.0, 4 mM ascorbate, 10 mM α -KG, 50 μ M Apo-ScoE, and 45 μ M (NH₄)₂Fe(SO₄)₂. After incubation, the assays are quenched by adding 50 μ L cold methanol, vortexed briefly, and centrifuged to remove protein residues. Time points are taken at 30 s, 1 min, 2 min, 5 min, and 15 min to determine the initial velocity of product formation. Product concentration is calculated by developing a standard curve using the INBA standard.

To determine the kinetic parameters of ScoE for α -KG, a Megazyme Succinate Assay kit was utilized to quantify succinate formation. The basic principle of the kit is that succinate produced by the ScoE reaction (α -KG cleavage) will be converted to succinyl-CoA in the presence of adenosine triphosphate (ATP) and coenzyme A (CoA) by the enzyme succinyl-CoA synthetase, which also produces ADP and inorganic phosphate. ADP and phosphoenolpyruvate (PEP) are then converted to pyruvate and ATP by pyruvate kinase. Lastly, lactate dehydrogenase (LDH) converts pyruvate and nicotinamide adenine dinucleotide (NADH) to lactate and NAD⁺. Notably, the amount of succinate is stoichiometric with the amount of NAD⁺ that can be estimated by measuring the absorbance decrease at 340 nm. Biochemical assays were performed in triplicate in a 96 well plate. The assays consisted of 50 µL containing 4 mM ascorbate, 1 mM CABA, $2 \mu M$ Apo-ScoE, $1.8 \mu M$ (NH₄)₂Fe(SO₄)₂ and the components of the Megazyme succinate assay kit. The amount of α-KG was varied between the range of 10-500 µM. Initial velocities of succinate formation were determined by monitoring NADH oxidation at 340 nm at 15 s intervals for 20 min using a plate reader.



3. Mechanistic dissection of isonitrile formation using spectroscopic methods

3.1 NMR analyses of *in vitro* biochemical assays for detection of intermediates

After conducting a thorough investigation of the reaction products and stoichiometry, the main objective was to propose a plausible pathway for

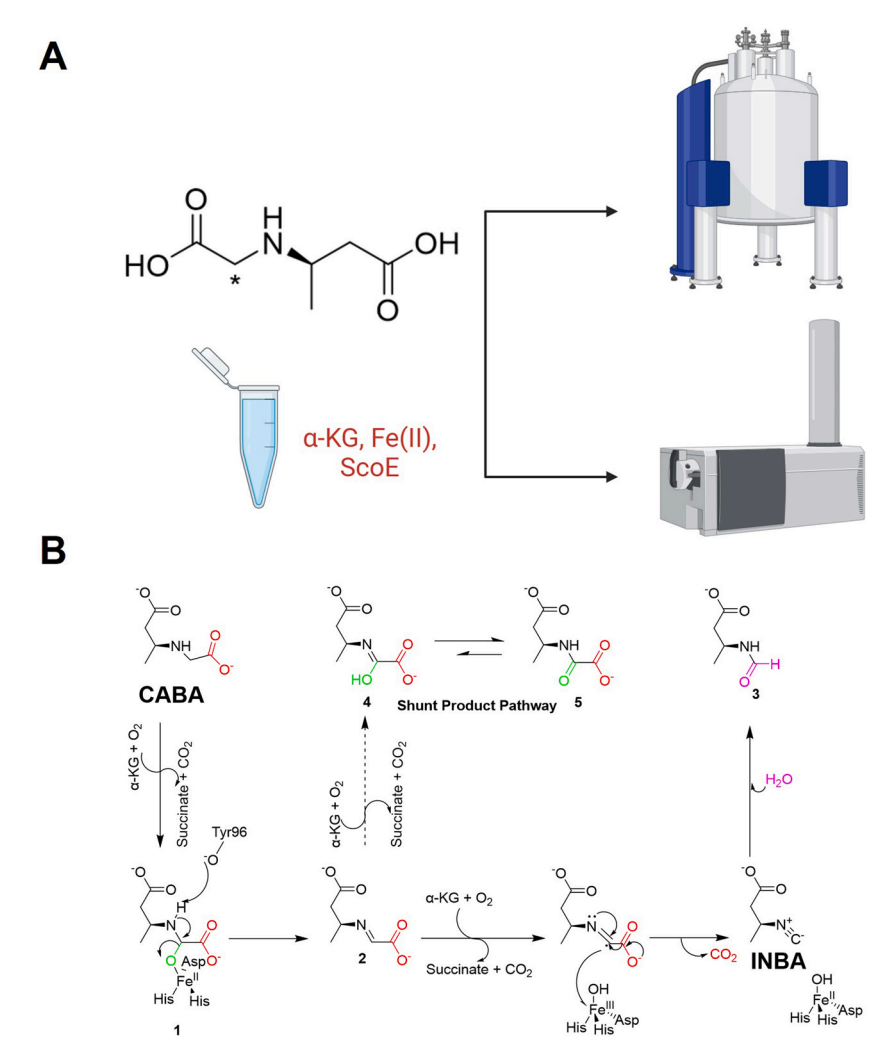


Fig. 3 Mechanistic dissection of isonitrile formation. (A) Research workflow employed to detect potential intermediates and shunt products from ScoE reaction. (B) Proposed mechanism for isonitrile formation by ScoE.

isonitrile formation with evidence for reaction intermediates (Del Rio Flores, Kastner, et al., 2022). Our first approach to address this challenge was to analyze the ScoE reaction utilizing nuclear magnetic resonance (NMR) at different time points to get an idea of the distinct species that are consumed and produced during the transformation towards isonitrile (Fig. 3A). With regards to developing an experimental plan, we reasoned

that utilizing a 5-13C version of CABA would help to minimize the signalto-noise ratio from NMR and allow for a better means to trace the reaction pathway. Another critical experimental parameter in designing this protocol is to perform these biochemical assays at 4 °C to slow down the enzymatic reaction to promote formation of intermediates. 5-13C-CABA can be chemically synthesized by reacting C2 with tert-butyl bromoacetate-2-13C and by following the rest of the synthetic scheme (Fig. 2). A 100 μL in vitro assay consisting of 50 mM HEPES pH 8.0, 4 mM 5-13C-CABA, 4 mM ascorbic acid, 150 µM Apo-ScoE, and 135 µM (NH₄)₂Fe $(SO_4)_2$ was incubated at 4 °C for 3 h and overnight, respectively. α -KG was added at a final concentration of 1.2 mM to initiate the reaction. The assay mixture was quenched with 100 µL of dimethyl sulfoxide (DMSO)-d₆ and dried under nitrogen. The experimentalist must ensure the reaction mixture is completely dry and this process can take several hours. The main reason to remove as much water as possible is to minimize the water peak signal from NMR. The contents were then resuspended to 140 µL of DMSO-d₆ and analyzed with NMR (i.e., ¹H, ¹³C, ¹H–¹³C heteronuclear single quantum coherence (HSQC), and ¹H-¹³C heteronuclear multiple bond correlation (HMBC)). As a negative control, it is important to repeat these two assays (3 h and overnight) using unlabeled CABA to "subtract" the background from NMR spectra with labeled substrate. Our unlabeled assay NMR spectra sample contained various signals that were assigned to α-KG, succinate, HEPES, ascorbic acid, and (6S,6aR)-3,3,3a,6-Tetrahydroxytetrahydrofuro[3,2-b]furan-2(3H)-one (oxidized form of ascorbic acid) (Del Rio Flores, Kastner, et al., 2022). Our 3-h assay revealed two new enriched correlations in HSQC and one new enriched correlation in HMBC, respectively, that were absent from the unlabeled CABA control. These correlations were assigned to originate from C5 of 1, 2, and INBA, respectively based on our synthetic standards (Fig. 3B). For our overnight assay, we observed disappearance of the signal associated with 1, but we were still able to detect the associated signals with 2 and INBA. Furthermore, we also observed an additional HSQC correlation and two HMBC correlations that we assigned to compounds 3, 4, and 5 based on comparisons to synthetic standards, LC-HRMS analyses, and computational analyses (Del Rio Flores, Kastner, et al., 2022) (Fig. 3B). The take-home message from this NMR strategy is after identifying the compounds produced from the enzymatic reaction, it becomes necessary to discern between reaction intermediates, shunt products, and degradation pathways as we will outline in 3.3.

3.2 Chemical synthesis of reaction intermediates and shunt products

After detecting NMR correlations that were putatively assigned to originate from C5 of 1-5, our objective was to chemically synthesize as many of these species as possible (Del Rio Flores, Kastner, et al., 2022) (Fig. 4). In practice, we formulated a hypothesis for the identity of these intermediates/shunt products due to our LC-HRMS analyses (described in the next section) and knowledge that isonitriles decompose in aqueous environments to generate formamides (Hagadone, Scheuer, & Holm, 1984; Iengo, Santacroce, & Sodano, 1979; Massarotti, Brunelli, Aprile, Giustiniano, & Tron, 2021) (INBA conversion to 3). Attempts to synthesize 1 and 4 were unsuccessful due to their instability and inherent propensity to tautomerize or become hydrolyzed. We focus our attention on this section to synthesis of compounds 2, 3, and 5. After verifying the structures with NMR, we compared the C5 carbon signals from these compounds to the NMR spectra from the previous section to verify our hypotheses. Furthermore, these three compounds can be utilized as primary substrates for ScoE biochemical assays to test for their potential intermediacy. Our results showed that only 2 can be converted to INBA by ScoE based on LC-HRMS analyses (Del Rio Flores, Kastner, et al., 2022).

(R)-3-aminobutanoic acid (2.08 g, 20 mmol) is dissolved in 50 mL of methanol in a round bottom flask with a magnetic stir bar and cooled to 0 °C. SOCl₂ (1.43 g, 12 mmol) is added dropwise as the mixture is being stirred at 0 °C. After a 30-min incubation period at 0 °C, the mixture is refluxed using a condenser for 5 h. The organic solvent is then removed *in vacuo* using a rotary evaporator to yield **A2**, a clear oil (95% yield, 1.98 g).

A2 (0.42 g, 4 mmol) was dissolved in 100 mL of tetrahydrofuran (THF) in a round bottom flask with a magnetic stir bar. Triethylamine (0.82 mL, 6 mmol) was added at room temperature, followed by addition of ethyl chlorooxoacetate (0.9 mL, 8 mmol). The reaction flask is heated to 50 °C and stirred for 8 h. The mixture is cooled down to room temperature and quenched with the same volume of water. The mixture is extracted with ethyl acetate and the water layer is washed three times. The organic fractions are washed with brine three times, dried with Na₂SO₄, and the ethyl acetate is removed in *vacuo* using a rotary evaporator to yield **A3**, a yellow oil (72% yield, 0.3 g).

A3 (0.22 g, 1 mmol) is mixed with 1 mmol KOH, 3 mL THF, and 0.6 mL H2O in a round bottom flask with a magnetic stir bar. The mixture

Fig. 4 Synthetic schemes for compounds 2, 3, and 5.

is then stirred at room temperature for 5 h, followed by removal of the organic solvent *in* vacuo using a rotary evaporator. The extract is next dissolved in 10 mL of ethyl acetate and 10 mL of water. The water layer is separated and washed with ethyl acetate three times. The water is lastly removed in *vacuo* using a rotary evaporator to yield **5** as a potassium salt (70% yield, 0.15 g).

I1 (0.39 g, 2 mmol) is mixed with 1 mmol KOH, 3 mL THF, and 0.6 mL of water in a round bottom flask with a magnetic stir bar. The mixture is stirred at room temperature for 5 h, followed by removal of the organic solvent in *vacuo* using a rotary evaporator. The resulting extract is subsequently dissolved in 10 mL ethyl acetate and 10 mL water. The water layer is separated and washed with ethyl acetate three times. The water is finally removed *in vacuo* using a rotary evaporator to yield **3** as a potassium salt (60% yield, 0.23 g).

A2 (0.42 g, 4 mmol) is first dissolved in 7 mL of anhydrous DCM, followed by addition of Na₂SO₄ (3 g, 21 mmol) in a round bottom flask containing a magnetic stir bar. Ethyl glyoxylate in 50% toluene (3.5 mL, 17.4 mmol) is added dropwise to the mixture and the reaction is stirred at room temperature for 18 h. The Na₂SO₄ was removed *via* filtration and DCM was subsequently removed *in vacuo* using a rotary evaporator. The remnants are dissolved in 10 mL ethyl acetate and 10 mL water. The water layer is washed with ethyl acetate three times and the organic fractions are pooled. The ethyl acetate is removed *in vacuo* using a rotary evaporator to yield **C1** as a yellow oil (45% yield, 0.2 g). When conducting this synthesis procedure, it is critical for the experimentalist to make sure the glassware is free of water. Also, ethyl glyoxylate must be appropriately stored at 4 °C and used within a month for best results.

C1 (0.1 g, 0.5 mmol) is charged with 0.5 mmol KOH, 3 mL THF, and 0.6 mL water in a round bottom flask containing a magnetic stir bar. The mixture is stirred at room temperature for 5 h, followed by removal of the organic solvent *in vacuo* using a rotary evaporator. The extract is subsequently dissolved in 10 mL ethyl acetate and 10 mL water. The water layer is separated and washed with ethyl acetate three times. The water is lastly removed *in vacuo* using a rotary evaporator to yield 2 as a potassium salt (53% yield, 50 mg).

3.3 LC-HRMS detection of intermediates and shunt products

In parallel to our NMR analyses with labeled CABA, we designed several biochemical assays that can be utilized to detect intermediates and shunt products from the ScoE biochemical reaction (Del Rio Flores, Kastner, et al., 2022). Each specific assay was utilized for a specific purpose, and we will outline in detail the potential use for each assay design.

The first assay involves performing a typical ScoE biochemical assay using half the normal amount of enzyme for short periods of time. A typical assay consists of $100\,\mu\text{L}$ of $50\,\text{mM}$ HEPES pH 8.0, $0.5\,\text{mM}$ CABA, $0.25\,\text{mM}$ α -KG, $50\,\mu\text{M}$ Apo–ScoE, and $45\,\mu\text{M}$ (NH₄)₂Fe(SO₄)₂ and is incubated at room temperature for 15 s, $30\,\text{s}$, 1 min, 1.5 min, 2 min, and 10 min. The enzymatic reaction is quenched with $200\,\mu\text{L}$ of cold methanol, gently mixed, and centrifuged for $10\,\text{min}$ to remove aggregated protein. LC–HRMS analysis is then conducted using the reaction supernatant. Through manual curation of the data, we were able to detect a metabolite with [M–H] = 174.0408 with a maximum MS intensity after overnight incubation that is not present in the negative controls. We designated this species to be Compound 4 and

not 5 since our synthetic standard of 5 had a different retention time. 4 was not consumed from the overnight time course, thus we assigned it as a shunt product. Lastly, we also detected compound 3 from the reaction mixture and was confirmed based on our synthetic standard. 3 was found to be a degradation product of INBA based on observation that our INBA standard partially degraded to 3. This analysis can be generalized further by conducting three replicate assays that are incubated at room temperature for 1.5 min, along with three replicate negative controls lacking iron. MS-dial is utilized to conduct comparative metabolomics analyses in both positive and negative ionization modes (Tsugawa et al., 2015) to identify compounds that are unique to the biochemical reactions and absent from negative controls. We obtained our hits by setting the following requirements: m/z: 100-200, abundance > 10^4 , t-test < 0.1, and reaction/negative control abundances > 1.

Although we were unable to detect 2 directly through LC-HRMS, we reasoned that we could identify the acid hydrolysis products of 2 based on the known instability of imines. We developed an assay for which we detected the degradation products of 2 to be (R)-3-aminobutanoic acid (R-3-ABA) and glyoxylate from ScoE assays that were derivatized with 2-nitrophenylhydrazine (2-NPH) after acidifying reactions with HCl. A time course was conducted to screen for formation of glyoxylate as a byproduct from acid hydrolysis of 2 and to determine the optimal incubation time. Typical biochemical assays consisted of 100 µL of 50 mM HEPES pH 8.0, 1 mM CABA, 0.25 mM α -KG, 50 μ M Apo-ScoE, and 45 μ M $(NH_4)_2Fe(SO_4)_2$ and were incubated at room temperature for 30 s, 1 min, 2 min, and 30 min. The assay mixture is derivatized with $200\,\mu\text{L}$ of $16\,\text{mM}$ 2-nitrophenylhydrazine (2-NPH) dissolved in 1 mL of acetonitrile and 1 mL of 2 N HCl (He & Ryan, 2021). A glyoxylate standard was subjected to the same derivatization scheme for comparison. The derivatization reaction was incubated at room temperature for 30 min, followed by centrifugation for 10 min to remove protein aggregates. The ScoE reaction and glyoxylate synthetic standard generated derivatized E- and Z-isomers of glyoxylate with matching retention times, subject to negative controls. Future assays were performed for a 1-min incubation time as the maximum amount of derivatized E- and Z-isomers of glyoxylate were detected. One can also utilize 5-13C-CABA and 6-13C-CABA in place of CABA with the same assay conditions as controls since there should be a mass spectral shift of +1. Note that the amount of α -KG was chosen to be 4 times less than CABA to enhance production of 2 and prevent excess conversion to INBA.

The last species that we detected from our NMR analyses was the transient C5-OH species 1, although we were unsuccessful at detecting this species though LC-HRMS. Based on the transient nature of 1, we proposed that it was the first intermediate in the isonitrile pathway with the first halfreaction of α-KG generating an Fe(IV)=O species, followed by C5-H abstraction and hydroxylation to yield 1. A catalytic base near the active site was proposed to aid in the subsequent dehydration of 1 to form 2. We hypothesized that Tyr96, which forms a hydrogen bond with the CABA amine would play the role of a base. Our previous biochemical characterization of the Y96F ScoE mutant revealed that it was unable to synthesize INBA from CABA. Furthermore, we used the previous glyoxylate derivatization assay with Y96F ScoE and found that it was able to generate succinate from α -KG together with a trace amount of 2, which was likely generated from dehydration of 1 halted at the active site. Altogether, we were able to propose a plausible reaction pathway towards isonitrile formation that supported our spectroscopic and computational analyses.

3.4 Kinetic and quantitative dissection of on-pathway and offpathway species

The isonitrile-forming mechanism of ScoE is a complex enzymatic pathway that generates various intermediates, shunt products, and degradation products (Del Rio Flores, Kastner, et al., 2022) (Fig. 3B). Several aspects of this enzymatic transformation draw tremendous interest from the enzymology community such as developing methods to quantify reaction products under certain conditions, while also understanding the relative kinetics for each step in the enzyme mechanism. Therefore, this section focuses on our recent efforts to dissect the kinetics and quantification of distinct species produced by ScoE *en route* to isonitrile formation.

First, we quantified the relative amounts of INBA, **2**, **3**, and **4** under conditions of limited and excess α -KG relative to CABA, respectively. Typical enzymatic assays consisted of 200 μ L containing 50 mM HEPES pH 8.0, 1 mM CABA, 1 mM α -KG, 50 μ M ScoE, and 45 μ M (NH₄)₂Fe (SO₄)₂, which were incubated at room temperature for 2 min. The reactions are split in half and the two fractions are subjected to the tetrazine click reaction and 2-NPH chemical derivatization, respectively. These assays are performed in triplicate experiments and more assays were performed with α -KG supplied in excess (3 mM). The fractions were then gently mixed, vortexed, and centrifuged to remove aggregated protein. The fractions that were derivatized with 2-NPH were utilized to indirectly

quantify the amount of 2 by detecting the degradation products of glyoxylate and R-3-ABA. The fraction modified by tetrazine was used to quantify the amounts of INBA, 3, and 4. Two sets of standards were prepared for the quantification of the reaction products. The first set consisted of 100 µL standards containing 50 mM HEPES pH 8.0 and varying concentrations of Py-AP, 3, and 5 (used to estimate amount of 4) that were subjected to the tetrazine click reaction. The second set consisted of 100 µL standards containing 50 mM HEPES pH 8.0 and varying concentrations of glyoxylate and R-3-ABA that were subjected to 2-NPH chemical derivatization. Biochemical assays and standards were analyzed using LC-HRMS. Standard curves were constructed from standard solutions to quantify the production of INBA, 2, 3, and 4. The amount of R-3-ABA and glyoxylate was found to be nearly identical, therefore the amount of 2 was subsequently estimated by quantifying production of glyoxylate. Our results showed that most reaction flux went towards forming INBA, but more 4 production was observed in conditions of excess α -KG.

Compound 2 was shown to be a catalytically competent intermediate towards INBA formation, therefore we developed a kinetic assay to determine the kinetic parameters of ScoE towards 2. 100 µL biochemical assays were performed in triplicate containing 50 mM HEPES pH 8.0, 3 mM α -KG, 50 μ M Apo-ScoE, and 45 μ M (NH₄)₂Fe(SO₄)₂. The reactions were initiated by adding α -KG and 2 was supplied at final concentrations of 10 µM, 50 µM, 100 µM, 2 mM, and 4 mM. Note that fresh 2 should be utilized for these assays since we observed rapid degradation of the compound even when stored at -80 °C for a week period. After incubation, the enzymatic reaction was quenched with 200 µL of 667 µM Py-tetrazine dissolved in cold methanol, gently mixed, and incubated for 1 h at room temperature. Time points were taken at 30 s, 1 min, 2 min, 5 min, and 15 min to determine the initial velocity of INBA formation. The product concentration was estimated by constructing a standard curve of Py-AP by analysis of standards containing 100 μL of 50 mM HEPES pH 8.0 and varying amounts of Py-AP.

Our final objective from our kinetic dissection of isonitrile formation was to develop a method to quantify the apparent rates of formation for compounds **2**, **3**, and **4** when utilizing CABA as a substrate. We designed $100 \,\mu\text{L}$ biochemical assays containing 50 mM HEPES pH 8.0, 1 mM CABA, 3 mM α -KG, $50 \,\mu\text{M}$ Apo-ScoE, and $45 \,\mu\text{M}$ (NH₄)₂Fe(SO₄)₂, which were incubated at room temperature to estimate the rate of formation for compounds **2**, **3**, and **4**. Time points were taken at $30 \, \text{s}$, 1 min,

2 min, 10 min, and 20 min to monitor the formation of 2 and 4. Time points were taken at 10 min, 1.5 h, 3 h, 6 h,18 h, and 26 h to monitor the formation of 3. After incubation, the enzymatic reactions used to detect 3 and 4 were quenched with 200 µL of cold methanol, gently mixed, and vortexed. The enzymatic reactions used to detect 2 were quenched with 2-NPH. A pseudo-first order kinetic model was utilized for each species to estimate the rate constant of formation. Standard curves were constructed as mentioned earlier in this section to quantify the amounts of 2, 3, and 4. Our kinetic analyses showed that the formation of 2 from CABA was much faster than the conversion of 2 to INBA, thus suggesting that the second half-reaction involving the transformation of 2 to INBA is rate-limiting. In addition, these kinetic analyses supported that the degradation and shunt pathways do not outcompete the main pathway towards isonitrile formation.



4. Enzyme expression, purification, and in vitro assays with Rv0097

4.1 Expression and purification of soluble protein

Rv0097 is a homolog of ScoE (45% sequence identity/61% sequence similarity) from *Mycobacterium tuberculosis* that also possesses the ability to generate isonitrile from CABA analogs, although with a fatty-acyl chain preference of > C10 (Del Rio Flores et al., 2023). The same general procedure for protein expression and purification that was described for ScoE can be applied to Rv0097. A notable difference in the expression protocol is that we observed improved production of Rv0097 when inducing with IPTG at an OD₆₀₀ of 0.6 compared to 0.5–0.6 for ScoE. Furthermore, we found that adding Ni–NTA at 3 mL/L of culture resulted in better isolation of Rv0097 from the purification process. Depending on different expression levels, the purity of Rv0097 ranges from ~80–95%. Ion exchange and size exclusion chromatography can be employed to further purify resulting protein.

4.2 Chemical synthesis of substrate

The native substrates of Rv0097 are not commercially available, therefore the analyst must synthesize the compounds prior to conducting biochemical assays, along with the isonitrile products (Del Rio Flores et al., 2023). The precursors and solvents are acquired from commercial vendors, including Enamine, Sigma-Aldrich, and Cambridge Isotope Laboratories.

We reconstituted the activity of Rv0097 using the surrogate substrate CADA (3-[(carboxymethyl)amino]decanoic acid) due to prior availability of the precursor molecule (3-aminodecanoic acid). Notably, our 3-aminodecanoic acid from Enamine contains a mixture of R and S isomers, instead of a single R isomer that was used to synthesize CABA. The same general procedure for CABA and INBA synthesis can be followed to synthesize longer alkyl chain derivatives. One key difference in the synthetic strategy includes optimization of mobile phase when conducting flash column chromatography. When synthesizing CADA/INDA (C10), we found that utilizing a DCM/MeOH mobile phase instead of hexanes/ethyl acetate resulted in optimal isolation of our synthetic intermediates. CADA/INDA showed poor solubility in water, therefore it is recommended to dissolve both compounds in DMSO, especially if a longer alkyl chain derivative is synthesized.

4.3 Enzymatic synthesis of substrates

An alternative strategy to synthesize CABA analogs involves utilizing pathway enzymes (ScoBCD, Rv0098-0100) to enzymatically produce fatty-acyl chain substrates bearing a β-glycine adduct with varying fattyacyl chain length (Fig. 5) (Del Rio Flores et al., 2023). Typical reactions were conducted at room temperature for 2 h in 50 µL of 25 mM ammonium bicarbonate pH 7.8 containing 1 mM α , β -unsaturated fatty acid, 1 mM glycine, 5 mM ATP, 2 mM magnesium chloride (MgCl₂), 10 μM Rv0099, 20 µM Rv0100, and 30 µM Rv0098. After the incubation period, the assay is quenched with 200 µL of cold methanol, gently mixed, vortexed, and centrifuged for 10 min to remove aggregated protein. LC-HRMS is finally conducted to verify production of the CABA analog. Rv0098-0100 are utilized to produce longer alkyl chain substrates (C10-C16), while ScoBCD are utilized for synthesizing short to medium alkyl chain substrates (C4-C8). We typically run assays in parallel where glycine is replaced with labeled glycine (i.e., ¹⁵N-, 1-¹³C-, 2-¹³C-glycine) to ensure that we are producing the desired CABA analog. Notably, these coupled enzymatic assays can be combined with the product detection assays in the next section to enzymatically synthesize various alkyl chain length isonitrile compounds as previously done with ScoE, MmaE, and Rv0097 (Del Rio Flores et al., 2023). This method can potentially be utilized to probe the substrate specificities of other isonitrile-forming enzymes without the need for laborious chemical synthesis.

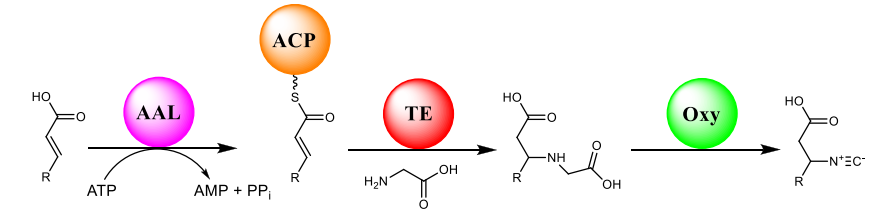


Fig. 5 Coupled enzymatic assay utilized to synthesize different fatty-acyl chain length CABA analogs by incubating α , β -unsaturated fatty acids and glycine with pathway enzymes. *AAL*, acyl-ACP ligase; *ACP*, acyl-carrier protein; *TE*, thioesterase; *Oxy*, Fe(II)/ α -KG dioxygenase.

4.4 Product detection assays

Similar to ScoE, activity assays with Rv0097 can be conducted to test for isonitrile production directly or via a click reaction with tetrazine to generate a stable derivatized product (Del Rio Flores et al., 2023). For the former case, when utilizing CADA as a substrate, we found that INDA can be directly detected in both positive and negative ionization modes with conventional reverse phase chromatography and mass spectrometry methods. However, it is recommended to utilize negative ionization mode due to the added benefit that you can detect α-KG and succinate. Typical activity assays are performed at room temperature for 15 min in 100 µL of 50 mM HEPES pH 8.0 containing 1 mM CADA, 2 mM α-KG, 100 μM Rv0097, and 90 μM (NH₄)₂Fe(SO₄)₂. The reactions are quenched with 200 µL of cold methanol after the incubation period and analyzed with LC-HRMS. Negative controls should be performed, and enzymatic products are compared to a synthetic INDA standard and commercially purchased succinate. For the case of a click reaction, 200 µL of 667 µM Pytetrazine is used to quench the reaction, followed by gentle mixing and incubation for 1 h at room temperature. The quenched reaction mixture is then centrifuged for 10 min to remove aggregated protein and analyzed with LC-HRMS. Similar to the case with ScoE, a synthetic standard of Py-AP is used for comparison of retention time and mass spectra.

4.5 Kinetic characterization of Rv0097

The kinetic characterization of Rv0097 was conducted to find the kinetic parameters for CADA but this general procedure can be applied to other analogs/potential substrates as described in this section (Del Rio Flores et al., 2023). A LC-HRMS assay was designed in which CADA concentration is varied, while the relative amount of α -KG is kept in excess

(Del Rio Flores et al., 2023). Biochemical assays ($100\,\mu\text{L}$) are performed in triplicate containing 50 mM HEPES pH 8.0, 5 mM α -KG, 50 μ M ApoRv0097, and 45 μ M (NH₄)₂Fe(SO₄)₂. The reactions were initiated by addition of α -KG, and CADA was supplied at final concentrations between 50 μ M and 4 mM. After incubation, the enzymatic reactions are quenched with 200 μ L of 667 μ M Py-tetrazine dissolved in cold methanol, gently mixed, and incubated for 1 h at room temperature. The subsequent reactions were centrifuged to remove protein debris and the supernatant was analyzed with LC–HRMS. Time points were taken at 30 s, 1 min, 2 min, 5 min, and 10 min to determine the initial velocity of INDA formation. The product concentration was estimated by constructing a standard curve of Py-AP by analysis of standards containing 100 μ L of 50 mM HEPES pH 8.0 and varying amounts of Py-AP that were also quenched with 200 μ L of 667 μ M Py-tetrazine. A Megazyme Succinate Assay kit can also be utilized if the goal is to determine the kinetics of Rv0097 for α -KG.

5. Perspectives

Our in-depth characterization of the INLP pathway in Actinobacteria, particularly for isonitrile formation by Fe/α-KG dioxygenases, revealed critical insight into the reaction mechanism and substrate specificity of isonitrile-forming enzymes, thus opening doors for potential engineering applications. The isonitrile-forming pathway of ScoE and its homologs has been the subject of many mechanistic and biosynthetic studies to date, yet advances toward implementing isonitrile enzymatic machinery to produce novel isonitrile-containing small molecules remains limited (Bunn, Xu, Webb, & Viswanathan, 2021; Del Rio Flores et al., 2023; Harris et al., 2017; Ittiamornkul et al., 2015; Wong, Mokkawes, & De Visser, 2022). Our characterization of the INLP pathway in Streptomyces and Mycobacteria revealed that homologous pathway enzymes have different, but relaxed substrate specificities towards different alkyl chain lengths. Therefore, it is interesting to probe the possibility of using promiscuous natural product biosynthetic enzymes to incorporate an isonitrile precursor into different major classes of natural products such as polyketides, lipopeptides, and hybrid systems. A key consideration for future engineering efforts will involve understanding and improving the tolerance of downstream megasynthases toward the isonitrile group, as well as protein-protein interactions between isonitrile carriers (ScoB homologs) and enzyme partners (i.e., NRPS, PKS)

since these interactions may also play an important role in channeling the isonitrile precursor to targeted downstream enzymes for the efficient biosynthesis of isonitrile-containing natural products.

Acknowledgments

The relevant research in the Zhang lab was financially supported by grants to W.Z. from the NIH (R01GM136758 and R35GM153289). A.D.R.F. was financially supported by the Blavatnik Innovation Fellowship and UC Berkeley Chancellor's Fellowship.

References

- Blasiak, L. C., Vaillancourt, F. H., Walsh, C. T., & Drennan, C. L. (2006). Crystal structure of the non-haem iron halogenase SyrB2 in syringomycin biosynthesis. *Nature*, 440(7082), 368–371. https://doi.org/10.1038/nature04544.
- Bollinger, J. M., Price, J. C., Hoffart, L. M., Barr, E. W., & Krebs, C. (2005). Mechanism of taurine: α-Ketoglutarate dioxygenase (TauD) from Escherichia coli. European Journal of Inorganic Chemistry, (21), 4245–4254. https://doi.org/10.1002/ejic.2005004.
- Brady, S. F., Chao, C. J., Handelsman, J., & Clardy, J. (2001). Cloning and heterologous expression of a natural product biosynthetic gene cluster from eDNA. *Organic Letters*, (6), 20–23. https://doi.org/10.1021/ol015949k.
- Brady, S. F., & Clardy, J. (2005). Cloning and heterologous expression of isocyanide biosynthetic genes from environmental DNA. Angewandte Chemie—International Edition, 44(43), 7063–7065. https://doi.org/10.1002/anie.200501941.
- Buglino, J. A., Ozakman, Y., Xu, Y., Chowdhury, F., & Glickman, M. S. (2022). Diisonitrile lipopeptides mediate resistance to copper starvation in pathogenic mycobacteria. MBio, 13(5), 1–14. https://doi.org/10.1128/mbio.02513-22.
- Bunn, B. M., Xu, M., Webb, C. M., & Viswanathan, R. (2021). Biocatalysts from cyanobacterial hapalindole pathway afford antivirulent isonitriles against MRSA. *Journal of Biosciences*, 46(2), 1–13. https://doi.org/10.1007/s12038-021-00156-4.
- Chang, W., Sanyal, D., Huang, J., Ittiamornkul, K., Zhu, Q., & Liu, X. (2017). In vitro stepwise reconstitution of amino acid derived vinyl isocyanide biosynthesis: Detection of an elusive intermediate. Organic Letters, 19, 1208–1211. https://doi.org/10.1021/acs.orglett.7b00258.
- Clarke-Pearson, M. F., & Brady, S. F. (2008). Paerucumarin, a new metabolite produced by the pvc gene cluster from Pseudomonas aeruginosa. *Journal of Bacteriology*, 190(20), 6927–6930. https://doi.org/10.1128/jb.00801-08.
- Crawford, J. M., Portmann, C., Zhang, X., Roeffaers, M. B. J., & Clardy, J. (2012). Small molecule perimeter defense in entomopathogenic bacteria. *Proceedings of the National Academy of Sciences of the United States of America*, 109(27), 10821–10826. https://doi.org/10.1073/pnas.1201160109.
- Del Rio Flores, A., Barber, C. C., Narayanamoorthy, M., Gu, D., Shen, Y., & Zhang, W. (2022). Biosynthesis of isonitrile- and alkyne-containing natural products. *Annual Review of Chemical and Biomolecular Engineering*, 13(1), 1–24. https://doi.org/10.1146/annurev-chembioeng-092120-025140.
- Del Rio Flores, A. W., Kastner, D., Du, Y., Narayanamoorthy, M., Shen, Y., Cai, W., ... Zhang, W. (2022). Probing the mechanism of isonitrile formation by a non-heme iron (II)-dependent oxidase/decarboxylase. *Journal of the American Chemical Society*, 144(13), 5893–5901. https://doi.org/10.1021/jacs.1c12891.
- Del Rio Flores, A., Narayanamoorthy, M., Cai, W., Zhai, R., Yang, S., Shen, Y., ... Zhang, W. (2023). Biosynthesis of isonitrile lipopeptide metallophores from pathogenic mycobacteria. Biochemistry, 62(3), 824–834. https://doi.org/10.1021/acs.biochem.2c00611.

- Drake, E. J., & Gulick, A. M. (2008). Three-dimensional structures of *Pseudomonas aeru-ginosa* PvcA and PvcB, two proteins involved in the synthesis of 2-isocyano-6,7-dihydroxycoumarin. *Journal of Molecular Biology*, 384(1), 193–205. https://doi.org/10.1016/j.jmb.2008.09.027.
- Grzyska, P. K., Appelman, E. H., Hausinger, R. P., & Proshlyakov, D. A. (2010). Insight into the mechanism of an iron dioxygenase by resolution of steps following the FeIV=O species. Proceedings of the National Academy of Sciences of the United States of America, 107(9), 3982–3987. https://doi.org/10.1073/pnas.0911565107.
- Gu, D., & Zhang, W. (2022). Engineered biosynthesis of alkyne-tagged polyketides. Methods in Enzymology, 665, 347–373. https://doi.org/10.1016/bs.mie.2021.11.013.
- Hagadone, M. R., Scheuer, P. J., & Holm, A. (1984). On the origin of the isocyano function in marine sponges. *Journal of the American Chemical Society*, 106(8), 2447–2448. https://doi.org/10.1021/ja00320a044.
- Harris, N. C., Born, D. A., Cai, W., Huang, Y., Martin, J., Khalaf, R., ... Zhang, W. (2018). Isonitrile formation by a non-heme iron(II)-dependent oxidase/decarboxylase. *Angewandte Chemie—International Edition*, 57(31), 9707–9710. https://doi.org/10.1002/anie.201804307.
- Harris, N. C., Sato, M., Herman, N. A., Twigg, F., Cai, W., Liu, J., ... Zhang, W. (2017). Biosynthesis of isonitrile lipopeptides by conserved nonribosomal peptide synthetase gene clusters in Actinobacteria. *Proceedings of the National Academy of Sciences of the United States of America*, 114(27), 7025–7030. https://doi.org/10.1073/pnas.1705016114.
- He, H. Y., & Ryan, K. S. (2021). Glycine-derived nitronates bifurcate to O-methylation or denitrification in bacteria. *Nature Chemistry*, 13(6), 599–606. https://doi.org/10.1038/ s41557-021-00656-8.
- Huang, Y. B., Cai, W., Del Rio Flores, A., Twigg, F. F., & Zhang, W. (2019). Facile discovery and quantification of isonitrile natural products via tetrazine-based click reactions. *Analytical Chemistry*. https://doi.org/10.1021/acs.analchem.9b05147.
- Huang, Y. B., Cai, W., Del Rio Flores, A., Twigg, F. F., & Zhang, W. (2020). Facile discovery and quantification of isonitrile natural products via tetrazine-based click reactions. *Analytical Chemistry*, 92(1), 599–602. https://doi.org/10.1021/acs.analchem. 9b05147.
- Iengo, A., Santacroce, C., & Sodano, G. (1979). Metabolism in Porifera. X. On the intermediary of a formamide moiety in the biosynthesis of isonitrile terpenoids in sponges. *Experientia*, 35(1), 10–11. https://doi.org/10.1007/BF01917842.
- Imming, P., Mohr, R., Muller, E., Overheu, W., & Seitz, G. (1982). [4 + 1]Cycloaddition of isocyanides to 1,2,4,5-tetrazines: a novel synthesis of pyrazole. *Angewandte Chemie*, 21(4), 284. https://doi.org/10.1002/anie.198202841.
- Ittiamornkul, K., Zhu, Q., Gkotsi, D. S., Smith, D. R. M., Hillwig, M. L., Nightingale, N., ... Liu, X. (2015). Promiscuous indolyl vinyl isonitrile synthases in the biogenesis and diversification of hapalindole-type alkaloids. *Chemical Science*, 6(12), 6836–6840. https://doi.org/10.1039/c5sc02919h.
- Jonnalagadda, R., Del Rio Flores, A., Cai, W., Mehmood, R., Narayanamoorthy, M., Ren, C., ... Drennan, C. L. (2021). Biochemical and crystallographic investigations into isonitrile formation by a non-heme iron-dependent oxidase/decarboxylase. *Journal of Biological Chemistry*, 296(Ii), 100231. https://doi.org/10.1074/jbc.ra120.015932.
- La Pierre, H. S., Arnold, J., Bergman, R. G., & Toste, F. D. (2012). Carbon monoxide, isocyanide, and nitrile complexes of cationic, d 0 vanadium bisimides: π-Back bonding derived from the π symmetry, bonding metal bisimido ligand orbitals. *Inorganic Chemistry*, 51(24), 13334–13344. https://doi.org/10.1021/ic302044q.
- Martinez, S., & Hausinger, R. P. (2015). Catalytic mechanisms of Fe(II)- and 2-oxoglutarate-dependent oxygenases. *Journal of Biological Chemistry*, 290(34), 20702–20711. https://doi.org/10.1074/jbc.R115.648691.

- Massarotti, A., Brunelli, F., Aprile, S., Giustiniano, M., & Tron, G. C. (2021). Medicinal chemistry of isocyanides. *Chemical Reviews*, 10742–10788. https://doi.org/10.1021/acs. chemrev.1c00143.
- Matsuda, K., Maruyama, H., Imachi, K., Ikeda, H., & Wakimoto, T. (2024). Actinobacterial chalkophores: The biosynthesis of hazimycins. *Journal of Antibiotics*, 2768, 228–237. https://doi.org/10.1038/s41429-024-00706-6.
- Mehdiratta, K., Singh, S., Sharma, S., Bhosale, R. S., Choudhury, R., Masal, D. P., ... Gokhale, R. S. (2022). Kupyaphores are zinc homeostatic metallophores required for colonization of *Mycobacterium tuberculosis*. *Proceedings of the National Academy of Sciences of the United States of America*, 119(8), 1–12. https://doi.org/10.1073/pnas. 2110293119
- Price, J. C., Barr, E. W., Glass, T. E., Krebs, C., & Bollinger, J. M. (2003). Evidence for hydrogen abstraction from C1 of taurine by the high-spin Fe(IV) intermediate detected during oxygen activation by taurine:α-ketoglutarate dioxygenase (TauD). *Journal of the American Chemical Society*, 125(43), 13008–13009. https://doi.org/10.1021/ja037400h.
- Rosano, G. L., & Ceccarelli, E. A. (2014). Recombinant protein expression in *Escherichia coli*: Advances and challenges. *Frontiers in Microbiology*, 5, 1–17. https://doi.org/10.3389/fmicb.2014.00172.
- Rui, Z., Li, X., Zhu, X., Liu, J., Domigan, B., Barr, I., ... Zhang, W. (2014). Microbial biosynthesis of medium-chain 1-alkenes by a nonheme iron oxidase. *Proceedings of the National Academy of Sciences of the United States of America*, 111(51), 18237–18242. https://doi.org/10.1073/pnas.1419701112.
- Schäfer, R. J. B., Monaco, M. R., Li, M., Tirla, A., Rivera-Fuentes, P., & Wennemers, H. (2019). The bioorthogonal isonitrile chlorooxime ligation. *Journal of the American Chemical Society*, 141, 18644–18648. https://doi.org/10.1021/jacs.9b07632.
- Stockmann, H., Neves, A. A., Stairs, S., Brindle, K. M., & Leeper, F. J. (2011). Exploring isonitrile-based click chemistry for ligation with biomolecules. *Organic and Biomolecular Chemistry*, 9, 7303–7305. https://doi.org/10.1039/c1ob06424j.
- Studier, F. W., & Moffatt, B. A. (1986). Use of bacteriophage T7 RNA polymerase to direct selective high-level expression of cloned genes. *Journal of Molecular Biology*, 189(1), 113–130. https://doi.org/10.1016/0022-2836(86)90385-2.
- Tsugawa, H., Cajka, T., Kind, T., Ma, Y., Higgins, B., Ikeda, K., ... Arita, M. (2015). MS-DIAL: Data-independent MS/MS deconvolution for comprehensive metabolome analysis. *Nature Methods*, 12(6), 523–526. https://doi.org/10.1038/nmeth.3393.
- Tu, J., Svatunek, D., Parvez, S., Liu, A. C., Levandowski, B. J., Eckvahl, H. J., ... Franzini, R. M. (2019). Stable, reactive, and orthogonal tetrazines: Dispersion forces promote the cycloaddition with isonitriles. *Angewandte Chemie—International Edition*, 58(27), 9043–9048. https://doi.org/10.1002/anie.201903877.
- Ugi, I., Werner, B., & Domling, A. (2003). The chemistry of isocyanides, their multicomponent reactions and their libraries. *Molecules*, 8, 53–66. https://doi.org/10.3390/80100053.
- Ushimaru, R., & Abe, I. (2023). Unusual dioxygen-dependent reactions catalyzed by nonheme iron enzymes in natural product biosynthesis. *ACS Catalysis*, 13(2), 1045–1076. https://doi.org/10.1021/acscatal.2c05247.
- Wang, Q., Wang, D., Wang, M., & Zhu, J. (2018). Still unconquered: Enantioselective passerini and ugi multicomponent reactions. *Accounts of Chemical Research*, 51, 1290–1300. https://doi.org/10.1021/acs.accounts.8b00105.
- Wang, L., Zhu, M., Zhang, Q., Zhang, X., Yang, P., Liu, Z., ... He, J. (2017). Dissonitrile natural product SF2768 functions as a chalkophore that mediates copper acquisition in Streptomyces thioluteus. ACS Chemical Biology, 12(12), 3067–3075. https://doi.org/10. 1021/acschembio.7b00897.

- Warui, D. M., Li, N., Nørgaard, H., Krebs, C., Bollinger, J. M., & Booker, S. J. (2011). Detection of formate, rather than carbon monoxide, as the stoichiometric coproduct in conversion of fatty aldehydes to alkanes by a cyanobacterial aldehyde decarbonylase. Journal of the American Chemical Society, 133(10), 3316–3319. https://doi.org/10.1021/ja111607x.
- Wong, H. P. H., Mokkawes, T., & De Visser, S. P. (2022). Can the isonitrile biosynthesis enzyme ScoE assist with the biosynthesis of isonitrile groups in drug molecules? A computational study. *Physical Chemistry Chemical Physics*, 121, 27250–27262. https://doi.org/10.1039/d2cp03409c.
- Zhang, X., Evanno, L., & Poupon, E. (2020). Biosynthetic routes to natural isocyanides. *European Journal of Organic Chemistry*, 2020(13), 1919–1929. https://doi.org/10.1002/ejoc.201901694.
- Zhi, S., Ma, X., & Zhang, W. (2019). Consecutive multicomponent reactions for the synthesis of complex molecules. *Organic and Biomolecular Chemistry*, 17, 7632–7650. https://doi.org/10.1039/c9ob00772e.
- Zhu, X., & Zhang, W. (2018). Terminal alkyne biosynthesis in marine microbes. *Methods in Enzymology*, 604, 89–112. https://doi.org/10.1016/bs.mie.2018.01.040.